Optimization of Design Parameters of Aircraft Wing Structure with Large Cut Outs using Damage Tolerant Design and Finite element analysis Approach

Thammaiah Gowda, Jagadeesha T, V.Dhinakaran

Abstract: ***Wings are the lift generating components in the airframe structure. Wings are also used as fuel tanks in the transport aircraft. Cutouts are provided in the bottom skin of the wing to permit entry into the airplane fuel tanks for inspection or component repair. Finite element method is adopted for stress analysis of the structural components. MSC NASTRAN and MSC PATRAN FEM packages are used to carry out the analysis. The damage tolerance capabilities of a wing box with a fuel access cutout to ensure the structural integrity while achieving the maximum possible safety margin and a reasonable lifetime of the aircraft structure is investigated. First finite Element Modeling of the Wing box in standard FE package (Global model) is carried out followed by structural analysis of the wing box to identify the critical location for fatigue crack initiation. Once critical location is found out, then Finite Element Modeling of the Panel with critical location for more detailed analysis (Local model) is carried out. Simulation of cracks of various lengths in the Local FE model and Stress intensity factor (SIF) calculations for each crack length using Modified Virtual Crack Closure Integral (MVCCI) method. Qualitative comparison of SIF with Fracture toughness for every crack length is carried.***

Index Terms: Stress concentration, Stress intensity factor, MVCCI, Finite element, Damage Tolerance.

I. INTRODUCTION

The wing contains fuel tanks and a cutout is provided to permit entry into the airplane fuel tanks for inspection or component repair. Hence it is called a fuel access cutout. Bottom skin is under tension stress field during flight. Cutouts are a geometrical discontinuity and give rise to stress concentration effect. Fatigue cracks get initiated due to high tensile stress due to discontinuity. Fig 1a shows Fuel tanks location in an aircraft Fig 1b shows right wing bottom view showing fuel access cutouts.

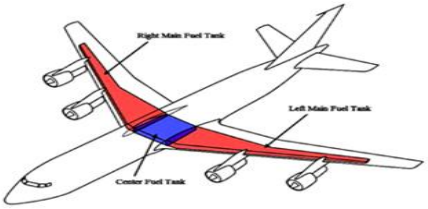

Fig. 1. a) Fuel tank locations in aircraft

Fig. 1. b) Cut out provided on wings of aircraft.

II. MODELING & ANALYSIS OF WING BOX

A. Modeling of Wing box: Global model

The wing consists of the spars, ribs, stringers, bottom skin and top skin. All the parts are modeled and assembled in CATIA and imported to MSC PATRAN. The wing box has two spars, each having a C shaped cross-section. The height of the spars taper from 182mm on the wing root side to 145mm on the wing tip side. The width of the spar flanges vary from 47mm on the wing root side to 40mm on the wing tip side. The thickness of the flange varies from 2.75mm on the wing root side to 2mm on the wing tip side. The web of the spar has uniform thickness of 3mm throughout. All the components of the wing box are made of, Aluminium Alloy, Aluminium– 2024-T351. The aircraft is designed for 3g conditions to withstand loads thrice its weight. For 3g condition the aircraft is designed to withstand 10000kgf or 98100N. 80% of the lift load is taken by the wings. Fig. 2 Shows the FEM model of wing box with boundary conditions.

Revised Manuscript Received on March 23, 2019.

Thammaiah Gowda, Principal, Yagachi Engineering College, Hassan, Karnataka state, India.
Dr. Jagadeesha, Assistant Professor, Department of Mechanical Engineering, National Institute of Technology Calicut, Kerala- 673 601
V. Dhinakaran, Department of Mechanical Engineering, Chennai Institute of Technology, Chennai -620 069, India

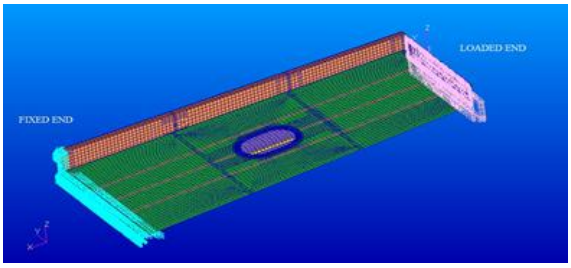

Fig. 2. Finite element model of wing portion with boundary conditions.

B. Load conditions

The span factor when multiplied by length of the wing gives the locations on the wing where the resultant loads can be considered to act. The load factor, when multiplied by the total load acting on one wing gives the magnitude of load acting at the corresponding locations on the wing found by multiplying span factor and length of that wing. The wing box under consideration is situated 2400mm away from the wing root end of the aircraft. The root end of the wing box in thus 9665-2400= 7265mm away from the free end of the wing.

C. Modeling of Wing box: Local Model

The location of maximum stress is the probable region for fatigue crack growth initiation. Thus for detailed analysis of damage tolerant capabilities of the wing box, a relevant local model (part of bottom skin) is considered for analysis.

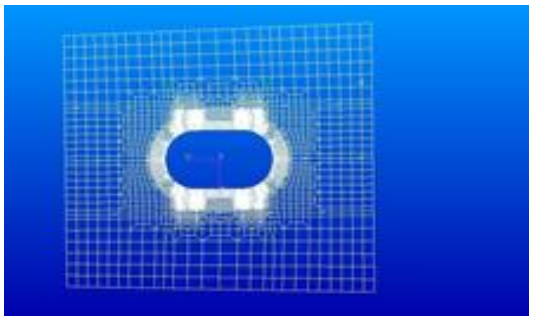

Fig. 3. a) Finite element model of cutout

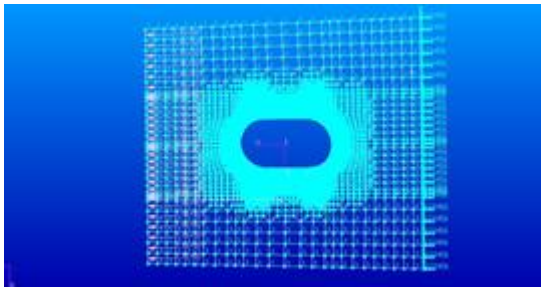

Fig. 3. b) Boundary conditions.

The meshing is carried out using 2D shell elements. the boundary condition for the local model can be considered as fixed at one end (near wing root) and tensile load acting on the other end (wingtip end) as shown in Fig.3. Also the translation in z direction is constrained in order to ensure the application of pure tensile load. Edge load on skin = 15.384 kg. Edge load on stringer‘s flange = 15.384 + 8.237 = 23.621 kg Edge load on stringer‘s web = 8.237 kg.On the application of the above edge loads the maximum value of stress obtained near the cutout was 14.6 kg/mm2 as opposed to 17.7 kg/mm2 in the global model

D. Modified Virtual Crack Closure Integral

Modified Virtual Crack Closure Integral (MVCCI) is a finite element based computation of strain energy release rate. By knowing the strain energy release rate we can calculate the Stress Intensity Factor (SIF). For the purpose of SIF calculation and Damage tolerance assessment, the detailed local model is used. The edge length of the elements in the crack path is maintained at 1.25mm. The crack is simulated using the split elements at nodes options under modify elements in the MSC PATRAN.

Cracks of different lengths are simulated; starting from 5mm, the length of the crack is incremented by 5mm for each iteration up to 55mm. From 55mm onwards, an increment of 1.25mm in the crack length is simulated. The SIF is calculated for each increment of crack length and compared to Fracture Toughness. Table 1 shows. FE data for SIF calculation for 5mm crack.

Table 1. FE data for SIF calculation for 5 mm crack.

Displacement	Differential displacment	GP force at node	GP force at Element	GP force (Kgf)	Total Force (Kgf)
0.42808260	0.02452010	75	48	53.57285	142.94
0.45260270			75	89.37	

III. RESULTS AND DISCUSSION

The results of the analysis of Global and local model under the corresponding boundary conditions and the damage tolerance capabilities of the wing box are disused below.

A. Maximum stress: Global Model

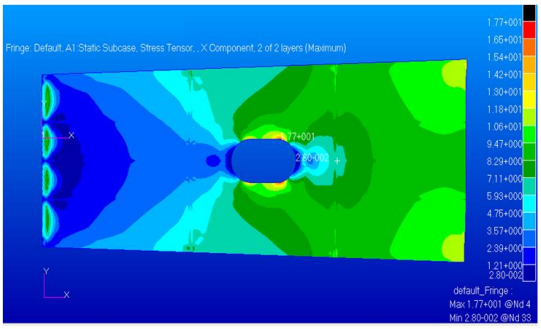

Fig. 4. Maximum stress distribution in Global model

The magnitude of maximum stress is 173.7MPa. The location of maximum stress is nearer to the fixed end as shown in Fig.4. This location can be treated as a probable region for fatigue crack initiation. The fuel access cutout has rivet holes provided for attaching the fuel access door. These rivet holes are not simulated in the global model for ease of analysis. But the representation of rivet holes is necessary for detailed and better results. This calls for the more detailed local analysis. A local model is created with rivet holes and the loading is simulated for a detailed investigation

B. Displacement: Global Model

The displacement of the wing box is shown in figure. The displacement can be explained through a cantilever beam analogy. In a cantilever beam with tip load, the maximum displacement is at the free end. The same applies here, i.e, the free end of the wing box experiences the maximum displacement. The maximum displacement in this case is 44mm.(Fig.5)

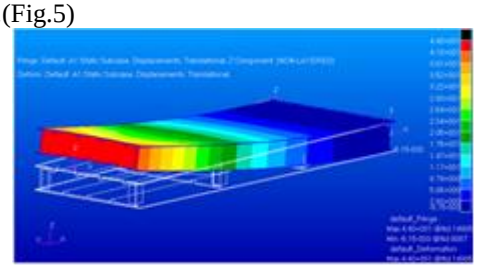

Fig. 5. Strain distribution in Global model

C. Maximum stress: Local Model

The boundary condition for the local model can be considered as fixed at one end (near wing root) and tensile load acting on the other end (wingtip end). Also the translation in direction is constrained in order to ensure the application of pure tensile load (Fig.6)

The figures show the portion which was considered for analysis i.e, the half part of the local model from the fixed end. Although the maximum stress in the effective local model is near the rivet hole, the replication of maximum stress from global model at the same location in local model as that location in global model proves that the right boundary conditions are used.

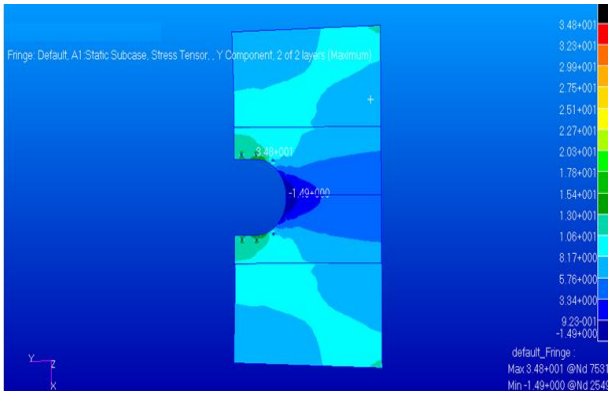

Fig. 6. Strain distribution in Global model

D. Displacement: Local Model

The displacement of the local model is similar to that of a plate subjected to axial load. The displacement at the fixed end is zero whereas the displacement at the free end is maximum. The displacement of the bottom skin under tensile loading is shown in the Fig.7. The maximum displacement is 1.29mm in y direction.

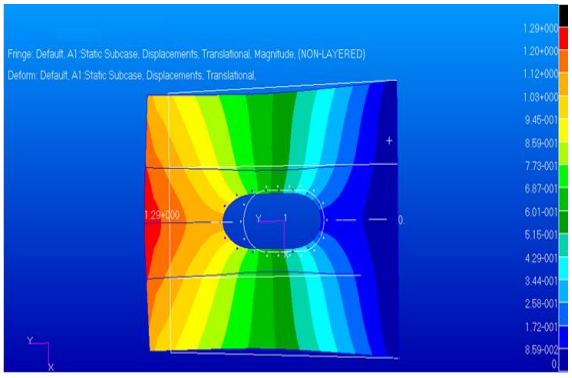

Fig. 7. Strain distribution in Global model

E. Damage Tolerance Evaluation

Damage tolerance evaluation is carried out by calculating stress intensity factor at crack tip for incremental crack lengths. The SIF calculated at every crack length will be compared with the fracture toughness of the material. For all crack lengths the elemental edge length Δa is maintained at 1.25mm. Displacements of opening nodes are obtained for each simulation of incremental cracks. Differential displacements near crack tip for a crack length of 60mm are shown in Table 2. Grid point forces are obtained for each simulation of incremental cracks and total grid forces is found to be 3922.23 N.

Table 2. Differential displacements near crack tip for a crack length of 60mm

Crack length	Displaced nodes	Displacement	Differential displacement
60 mm	287	0.48792030	0.07058100
	11567	0.55850130	

The variation of SIF (Stress Intensity Factor) as a function of crack length is shown in Fig.8. From that curvature of the graph it is evident that the SIF initially increases with the increasing length of the crack. The highest SIF value observed is 53.81 MPa√ m corresponding to a crack length of 50mm. When the crack extends beyond 50mm the SIF starts decreasing. This is because of the presence of stiffener (stringer) in the crack path. The stringer in the bottom skin is placed 60mm away from the cutout. Hence when the crack extends beyond 50mm, the crack tip is getting closer to the stiffener (stringer). The displacement at crack tip reduces near the stiffener, which results in decrease in strain energy release rate. Thus the SIF starts decreasing as the crack tip approaches the stringer. Stress Intensity Factor is compared with Fracture Toughness and is tabulated

İn Table 3

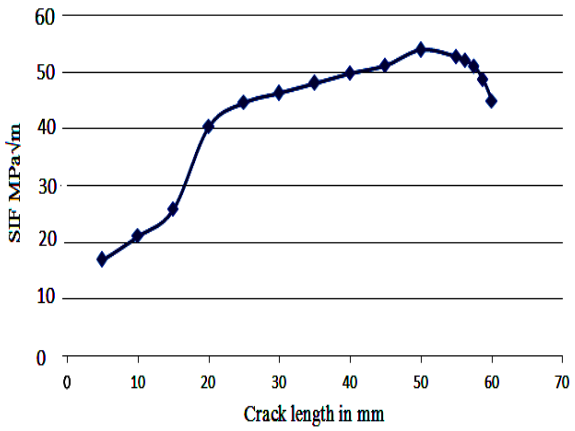

Fig. 8. Strain distribution in Global model

Table 3. Differential displacements near crack tip for a crack length of 60mm

Crack length (mm)	Thickness (mm)	Fracture Toughness	Stress intensity factor
5	3.5	95	16.87
10	3.5	95	21.04
15	3.5	95	25.77
20	3.5	95	40.26
25	3.0	97	44.29
30	3.0	97	46.21
35	3.0	97	47.21
40	3.0	97	47.90
50	2.5	98	53.81
55	2.5	98	52.57
57.5	2.5	98	50.86
60	4.0	93	44.77

It can be noted from the table that the SIF at any crack length does not exceed the fracture toughness. Thus the structure is safe. However maintenance must be carried out once the crack tip reaches the stringer (stiffener). This is to avoid the damage to stringer.

IV. CONCLUSIONS

In this work, the damage tolerance evaluation of wing box of a medium size transport aircraft having a large cutout in the bottom skin has been carried out. Finite element method was adopted for stress analysis of the structural components. MSC NASTRAN and MSC PATRAN FEM packages were used to carry out the analysis. The damage tolerance evaluation was carried out in steps. The stress analysis of the entire wing box under the 3g lift load condition was first carried out to identify the critical location for fatigue crack initiation. The critical location was found to be in the bottom skin of the wing. A local analysis was followed to obtain more accurate stress value and the distribution of stress. The maximum stress from the global model was simulated in the local model and at the same location as in the global model. The anomalies in the simulation could be neglected since the maximum stress and its location from global model was replicated in the local model. Hence it was considered sufficient that, only the portion where maximum stress from global model was replicated be considered for analysis.

The maximum stress in the local model was found near a rivet hole, close to the fixed end of the wing box. The stress in the rivet hole was found to be 341.388 N/mm2 (MPa). Since it is lesser than the tensile yield strength (The tensile yield strength of Aluminium 2024- T351 it is 345 MPa) the wing box can be considered safe for static strength under 3g loading conditions. The damage tolerance evaluation includes stress intensity factor for various crack lengths. The cracks of incremental length were simulated in the local model. The SIF was calculated for each crack length using Modified Virtual Crack Closure Integral (MVCCI) method which uses FE data like nodal displacements and grid point forces. The SIFs so calculated was compared with fracture toughness.

The SIF initially increased with the increasing length of the crack. When the crack extended beyond 50mm the SIF started decreasing. This is because of the presence of stiffener (stringer) in the crack path. The stringer in the bottom skin is placed 60mm away from the cutout. Hence when the crack extends beyond 50mm, the crack tip is getting closer to the stiffener (stringer). The displacement at crack tip reduces near the stiffener, which results in decrease in strain energy release rate. Thus the SIF starts decreasing as the crack tip approaches the stringer. For all lengths of crack the SIF remained below the fracture toughness. Thus the structure is safe. However maintenance must be carried out once the crack tip extends nearer to the stringer (for 58.75mm). This is to avoid the damage to stringer of an air craft.

REFERENCES

1. Micheal Chun., Yung Niu.: Airframe structural design, Practical design information and data on aircraft structures, Conmilit press, Hong Kong (2001).
2. Ralph I. Stephens., Ali Fatemi., Robert R., Stephens, Henry O. Fuchs: Metal Fatigue in Engineering, 2nd Edition, John Wiley (2000).
3. Pir M.Toor.: A review of some damage tolerance design approaches for aircraft structures, Engineering fracture mechanics, 5, 837-880 (1973).
4. Chiheb Chaker.: Stress trajectories in the presence of friction, International Journal of Solids and Structures, 40, 4033-4041 (2003).
5. Griffith, A.: The phenomena of rupture and flow in solids, Philosophical Transactions of the Royal Society, 163-198 (1921).
6. RamaChandra Murthy, A., Palani, G.S., Nagesh Iyer.: Damage tolerant evaluation of cracked stiffened panels under fatigue loading, Sadhana, 37, 171-186 (2012).
7. Sethuraman, R., Maiti,S.K.: Finite element based computation of strain energy release rate by modified crack closure integral, Engineering Fracture Mechanics,30,227-231 (1988).
8. Carlson,R.L.,Steadman, D.L.,Dancila.,D.S.: Fatigue growth of small corner cracks in aluminum 6061-T651. In:Proceedings of the FAA-NASA symposium on continued airworhiness of aircraft structures, pp.279-285,New York (1997).
9. Og Uzhan Demir., Ali O. Ayhan.: Evaluation of mixed mode criteria for fatigue crack propagation using experiments and modelling, Chinese Journalof Aeronautics, 31(7), 1525-1533 (2018).
10. Lin Lin., Luo Lin., Zhong.: Development and application of maintenance decision-making support system for aircraft fleet, Advances in Engineering Software, 114, 192-207 (2017).
11. Karthick, S., Devi, E.S., Nagarajan, R.V. “Trust-distrust protocol for the secure routing in wireless sensor networks”, In Proceedings of 2017 International Conference on Algorithms, Methodology, Models and Applications in Emerging Technologies, ICAMMAET 2017, 2017-January, pp. 1-5, 2017. DOI: 10.1109/ICAMMAET.2017.8186688

12. Karthick, S., Perumal Sankar, S., and Arul Teen, Y.P. "Trust-distrust protocol for secure routing in self-organizing networks", In Proceedings of 2018 International Conference on Emerging Trends and Innovations In Engineering And Technological Research, ICETIETR 2018, art. no. 8529016, 2018. DOI: 10.1109/ICETIETR.2018.8529016
13. Sathish, T., Periyasamy, P., Chandramohan, D., Nagabhooshanam, N. "Modelling K-Nearest Neighbour technique for the parameter prediction of cryogenic treated tool in surface rough minimization", International Journal of Mechanical and Production Engineering Research and Development, Special Issue, pp. 705-710, 2018.
14. Sathish, T., Muthukumar, K., Palani Kumar, B."A Study on Making of Compact Manual Paper Recycling Plant for Domestic Purpose", International Journal of Mechanical and Production Engineering Research and Development, Vol. 8, Special Issue 7, Dec 2018, pp. 1515-1535, 2018.
15. Sathish, T., and Karthick, S. "HAIWF-based fault detection and classification for industrial machine condition monitoring", Progress in Industrial Ecology, vol. 12, no. 1-2, pp. 46-58, 2018
16. Sathish, T., Muthulakshmanan, A. "Modelling of Manhattan K-Nearest Neighbor for Exhaust Emission Analysis of CNG-Diesel Engine", Journal of Applied Fluid Mechanics, Vol. 11, pp. 39-44, 2018,
17. Sathish, T., Periyasamy, P., Chandramohan, D., Nagabhooshanam, N. "Modelling of cost based optimization system E-O-L Disassembly in Reverse Logistics", International Journal of Mechanical and Production Engineering Research and Development, Special Issue, pp. 711-716, 2018.

AUTHORS PROFILE

Dr. Thammaiah Gowda is serving has Principal in Yagachi Engineering College, Hassan. He has published more than 50 papers in international and national journal and conferences. He has conducted several workshops and managed R and D projects. He is published two books.

Dr. Jagadeesha is working has assistant professor in the department of mechanical engineering at NIT Calicut

V Dhinakaran is Associate Professor in the Department of Mechanical Engineering, Chennai Institute of Technology, Chennai, Tamil Nadu, India. His area of research are welding, heat transfer, fluid mechanics and CFD.